TISSUE ENGINEERING: Part C
Volume 16, Number 5, 2010

DOI: 10.1089/ten.tec.2009.0760

Effects of Hyperinsulinemia on Lipolytic Function of Three-Dimensional Adipocyte/Endothelial Co-Cultures

Jennifer H. Choi, Ph.D.,[1] Jeffrey M. Gimble, M.D., Ph.D.,[2]
Gordana Vunjak-Novakovic, Ph.D.,[3] and David L. Kaplan, Ph.D.[1]

The increased incidence of both type 2 diabetes mellitus and obesity has prompted the need to develop physiologically relevant adipose tissue models for controlled study of both normal and diseased adipose functions. Insulin resistance, characteristic of both type 2 diabetes mellitus and obesity, is often preceded by hyperinsulinemia. We propose here a three-dimensional (3D) co-culture adipose tissue model to study the effects of high insulin exposure, which enabled the study of physiological cell responses to hyperinsulinemic conditions. Two-dimensional adipocyte studies were initially conducted to establish a baseline control in which insulin levels were established. Adipocytes and endothelial cells were subsequently co-cultured on 3D porous silk fibroin scaffolds in normal or high insulin concentrations, and their physiological responses were assessed with respect to lipogenesis and lipolysis. High insulin levels stimulated both an increase in triglyceride accumulation and a decrease in lipolysis levels compared to that of normal insulin conditions. In contrast, adipocyte monocultures did not exhibit any differences between insulin levels. The ability of this 3D system to elicit physiological responses to hyperinsulinemia in co-culture serves as a significant step forward in adipose tissue engineering. The development of physiologically relevant 3D *in vitro* adipose tissue models presents promise for the study of disease mechanisms as well as in assessing therapeutic treatments.

Introduction

The incidence of type 2 diabetes mellitus (T2DM) and obesity continues to increase around the world, adding to the already critical problem of cardiovascular disease.[1] In the United States alone, about two-thirds of adults are considered overweight or obese, and in the year 2000, 171 million individuals worldwide were estimated to have diabetes.[2] Therefore, much needs to be done to further our understanding of these diseases, toward the development of treatment options. Current treatment options for obesity consist of combinatorial therapies targeting weight loss, exercise, and a healthy diet.[3] T2DM has been associated with obesity, and the initial treatment regimes for T2DM include weight management therapies typically targeted for a 5%–10% reduction of body weight.[4] Additionally, the majority of T2DM patients also require pharmacotherapy. There are several classes of drugs that are currently being used for treatment of T2DM: agents to stimulate insulin production of β cells (sulfonylureas and meglitinides), drugs to decrease liver glucose production (biguanides and thiazolidinediones [TZDs]), dipeptidyl peptidase-4 (DPP) inhibitors, and α-glucosidase inhibitors.[5] Although current treatment options offer benefits in attaining glycemic control, complications include risks of hypoglycemia, weight gain, and decreased blood-glucose control over time.[4]

A characteristic of both T2DM and obesity is insulin resistance, defined by impaired insulin signaling and decreased insulin sensitivity.[6] Insulin resistance is also highly correlated with hyperinsulinemia.[7,8] Although insulin resistance is found in various tissues of the body, there is growing evidence that adipose tissue is among the first tissues to exhibit insulin resistance in the body.[1] In adipose tissue, insulin is a critical modulator of adipose function, in which it participates in adipogenic differentiation, glucose transport, triglyceride (TG) synthesis, and lipolysis inhibition.[6] Normal plasma insulin levels of insulin are in the range of 5–10 μU/mL (30–60 pM).[7,9,10] In the insulin-resistant state, normal insulin signaling is impaired, affecting adipocyte glucose uptake and metabolism.[6] Various studies have shown that hyperinsulinemia suppresses basal glycerol release from adipocytes and increases TG accumulation through increased glucose transporter-4 (Glut4) recruitment, and upon prolonged hyperinsulinemia, adipocytes become resistant to insulin as characterized by lowered glucose uptake and increased basal lipolysis.[11–13]

[1]Department of Biomedical Engineering, Tufts University, Medford, Massachusetts.
[2]Pennington Biomedical Research Center, Louisiana State University System, Baton Rouge, Louisiana.
[3]Department of Biomedical Engineering, Columbia University, New York, New York.

A number of two-dimensional (2D) culture and clinical studies have helped to develop an understanding of insulin resistance in adipose tissue, and of hyperinsulinemia.[12,14,15] The development of three-dimensional (3D) *in vitro* human tissue systems to further elucidate mechanisms involved in the disease in a controlled, physiologically relevant manner would offer a significant advancement in adipose tissue biology and in screening of potential new treatments. The utilization of 3D adipose tissue systems to study different physiological states provides several advantages over traditional 2D culture studies. The 3D environment provides a scaffold structure that functions as a more physiologically relevant microenvironment, promotes cell attachment and migration, and facilitates cell–cell and cell–matrix interactions.[16] Therefore, regenerative medicine strategies—more specifically, adipose tissue engineering—provide promising avenues for the study of adipose tissue in both the normal and diseased states. Common biochemical methods that have been used to measure adipose tissue functionality are presented in Figure 1. Key regulators of adipogenesis, as well as important variables involved with both lipogenesis and lipolysis are included.

In this study, we utilized a 3D adipose tissue system that we developed previously[17] based on tissue engineering strategies. The aim of the present work was to demonstrate that 3D co-culture provides a physiologically relevant setting for controlled study of hyperinsulinemia on lipolytic function. Specifically, our *in vitro* model consisted of co-culturing human adipocytes differentiated from human adipose-derived stem cells (hASCs) with human umbilical vein endothelial cells (HUVEC) on 3D porous silk scaffolds. Our experimental design consisted of 2D baseline studies and 3D cultures, specifically 3D hASC monocultures, HUVEC monocultures, and hASC/HUVEC co-cultures. The physiological response observed in the 3D co-cultures brings us another step forward in the development of a functionally relevant adipose tissue system.

Materials and Methods

Cell culture

hASCs were isolated according to published methods from subcutaneous adipose tissue donated with written consent by healthy volunteers undergoing elective liposurgery.[18] The work was reviewed and approved by the Pennington Biomedical Research Center Institutional Review Board. Isolated hASCs were cultured in Dulbecco's modified Eagle's medium (DMEM)/F-12 supplemented with 10% fetal bovine serum (FBS) and 1% antibiotic–antimycotic. Media were replenished every 3 days, and cells were passaged at 80% confluency using trypsin–EDTA and frozen using cell culture growth media containing 10% dimethyl sulfoxide. HUVECs were cultured according to company protocols. Briefly, HUVECs were expanded in endothelial growth medium (EGM) supplemented with EGM-bullet kit. Media were replenished every 2 days and followed the same passaging/freezing protocols as for the hASCs. hASCs seeded in 2D culture flasks were grown for 1 week in DMEM/F-12 media supplemented with 10% FBS and 1% penicillin–streptomycin (GM). Adipogenic differentiation was induced for 7 days in DMEM/F-12 media containing 3% FBS, 1% penicillin–streptomycin, 33 μM biotin, 17 μM pantothenate, 1 μM insulin, 1 μM dexamethasone, 500 μM 3-isobutyl-1-methyl-xanthine, and 5 μM TZD differentiation medium-Diff (Diff). Differentiated adipocytes were maintained in Diff minus 3-isobutyl-1-methyl-xanthine and TZD containing normal (1 μM) or high (10 μM) insulin levels maintenance medium (MM).

Preparation of aqueous silk scaffolds

Cocoons from *Bombyx mori* silkworm were supplied by Tajimia Shoji (Yokohama, Japan). Aqueous silk solution was prepared as previously described.[19] The resulting silk solution (7%–8% w/v) was further diluted to yield a 6% silk solution. Porous (500–600 μm pore size) aqueous silk scaffolds were prepared as previously described.[19] A biopsy punch was utilized to obtain final 4×2 mm (diameter×height) scaffolds.

DNA quantification

Scaffolds were harvested in TEX (10 mM Tris, 1 mM EDTA, and 1% triton X-100) and Proteinase K, and stored at −20°C. Samples were thawed, and incubated in 56°C water bath overnight for complete sample digestion. Samples were then chopped and centrifuged at 15,700 *g* for 10 min at 4°C, and supernatants were collected. DNA content was determined fluorometrically at 480/525 nm (ex/em) using an FLx800 spectrofluorometer (BioTek, Winooski, VT). The amount of DNA was determined by interpolation from a standard curve prepared using lambda DNA in 10 mM Tris-HCl (pH 7.4), 5 mM NaCl, and 0.1 mM EDTA over a range of concentrations.

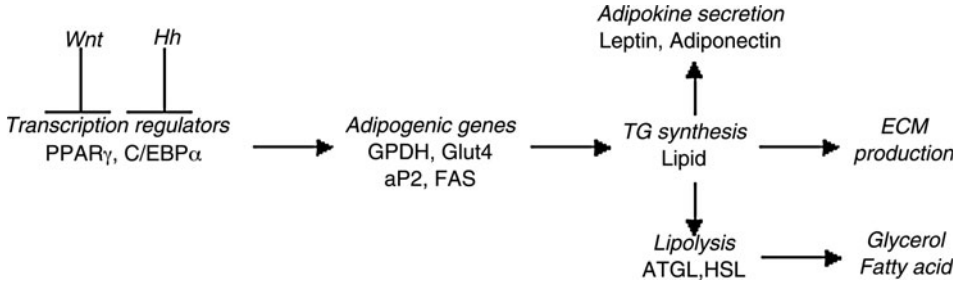

FIG. 1. Schematic of adipose tissue outcome measures. Adipogenic differentiation is initiated upon inhibition of both Wnt and Hedgehog (Hh) signaling. PPARγ and C/EBPα are key transcriptional regulators that promote expression of adipogenic genes such as *GAPDH*, *Glut4*, *FABP4*, and *ACS*. Triglyceride (TG) synthesis subsequently occurs, causing mature adipokines to be secreted (leptin and adiponectin) and extracellular matrix (ECM) production. TG breakdown, or lipolysis, is mediated by 2 key lipases (adipose triglyceride lipase [ATGL] and hormone sensitive lipase [HSL]), producing glycerol and fatty acids.

Lipid accumulation

Scaffolds were harvested in sodium dodecyl sulfate buffer (0.1% w/v) and stored at −20°C. At time of assay, samples were thawed, chopped, and sonicated briefly. After sonication, samples were centrifuged at 15,700 *g* for 10 min at 4°C, and supernatants were collected for assay. TG was measured using an enzymatic assay, in which a quinoneimine dye is produced proportional to glycerol, and quantified at 540 nm

Free glycerol secretion

Media samples were collected and stored at −80°C. Samples were thawed, and centrifuged at 15,700 *g* for 10 min at 4°C, and supernatants were collected. Detected glycerol was measured (540 nm) using the TG kit described earlier, however, excluding the hydrolysis step. Glycerol levels detected in medium samples from blank scaffolds were subtracted from all medium samples.

Real-time reverse transcription-polymerase chain reaction

Total RNA was extracted from cells using Trizol reagent. Scaffolds harvested in Trizol were stored at −80°C. After thawing, scaffolds were chopped and centrifuged at 15,700 *g* for 10 min at 4°C. Supernatants were transferred to new tubes, and RNA was isolated according to supplier's instructions. Reverse transcription was performed using high-capacity cDNA reverse transcription kit following supplier's instructions. Commercially available primers and probes from TaqMan® Gene Expression Assays were utilized for target genes *Glut4* and platelet-endothelial cell adhesion molecule (*CD31*), and normalized to the housekeeping gene, *GAPDH*, using the $2^{\Delta\Delta Ct}$ formula. Specifically, real-time reverse transcription (RT)-polymerase chain reactions were performed using an ABI 7500 Sequence Detection System (Applied Biosystems, Foster City, CA) at 50°C for 2 min, 95°C for 10 min, followed by 40 cycles of amplifications, consisting of a denaturation step at 95°C for 15 s, and extension step at 60°C for 1 min.

Experimental design

Preliminary 2D studies were conducted to establish the ability of hASCs to respond to normal MM containing 1 μM insulin, and to hyperinsulinemic MM containing 10 μM insulin. Phase-contrast images were collected to investigate morphological changes, and free glycerol secretion quantified as measure of basal lipolysis in both insulin conditions.

Three-dimensional studies were then conducted in which HUVECs were seeded on silk scaffolds (500,000 cells/scaffold) on day 0. Seven-day-differentiated adipocytes (235,000 cells/scaffold) were added to HUVEC-seeded scaffolds 1 week later. After 3 days (considered as day 0 in this experiment), the medium was exchanged to either normal MM containing 1 μM insulin or to hyperinsulinemic MM containing 10 μM insulin. Control cultures included adipocyte monocultures and endothelial monocultures, in which the number of each cell type was equivalent to the number seeded in co-culture (i.e., adipocyte monocultures were seeded with 235,000 cells/scaffold, and endothelial monocultures with 500,000 cells/scaffold). All scaffolds were cultured in 1:1 EGM:MM media, and media exchanged every 3 days. On days 0, 3, 6, and 9, samples were collected for DNA content, TG quantification, and free glycerol secretion, and evaluated for specific gene expression levels. On day 9, the medium of hyperinsulinemic samples was exchanged for normal MM containing 1 μM insulin, and cultured for an additional 3 days.

Statistical analysis

All reported values were averaged ($n = 3$) and expressed as mean ± standard deviation. Statistical differences were determined using Student's two-tailed *t*-test and differences were considered statistically significant at $p < 0.05$.

Results

Hyperinsulinemic effects on 2D hASC culture

In a baseline study, hASCs were differentiated for 7 days in 2D and subsequently cultured in a medium containing 1 or 10 μM insulin for 12 days. Phase-contrast images were taken as a preliminary screen of differentiated adipocyte morphology and lipid content (Fig. 2). Differentiated adipocytes cultured in 1 μM insulin accumulated lipid as shown through phase-contrast images. The hASCs changed from fibroblastic-like morphology to a rounded morphology, in which adipocytes were found in clusters throughout the

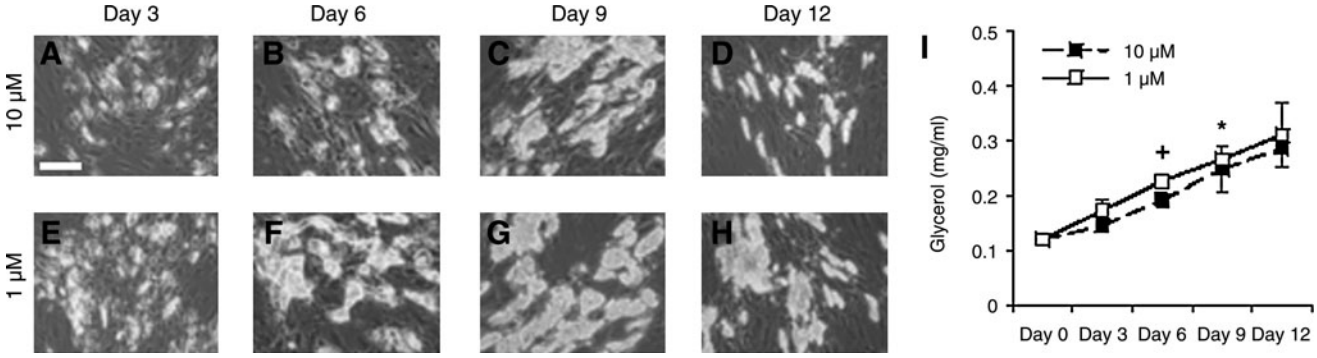

FIG. 2. Two-dimensional adipogenic-differentiated hASCs. hASCs were cultured for 12 days in the medium containing 10 μM insulin (**A–D**) or 1 μM insulin (**E–H**) ($n = 3$), and secreted glycerol (mg/mL) was measured at each time point (**I**). Scale bar = 50 μm. Original magnification, 10×. Significant difference between insulin levels are labeled as $^{+}p < 0.05$; significant differences from day 0 levels are labeled as $^{*}p < 0.05$.

culture well with time. Additionally, images displayed increased intracellular lipid content with time, contributing to the increase in adipocyte size. Adipocytes cultured in high insulin media (10 μM) also exhibited similar changes in morphology with time in addition to increased lipid content after 9 days culture. However, at 12 days, intracellular lipid content decreased as evident by decreased cell size and less clustering of adipocytes.

Basal lipolysis of differentiated adipocytes cultured in 1 μM or 10 μM insulin was measured through secreted glycerol quantification (Fig. 2I). Secreted glycerol levels were greater in 1 μM adipocytes at each time point compared with 10 μM adipocytes; however, a significant difference was noted only at day 6 ($^{+}p < 0.05$). Adipocytes cultured in both 1 or 10 μM insulin secreted increased glycerol with time ($^{*}p < 0.05$).

Proliferation of 3D adipocyte mono and co-cultures

The 3D constructs consisted of hASC monocultures, HUVEC monocultures, and hASC/HUVEC co-cultures. DNA content in 3D constructs was measured over 12 days for both normal and hyperinsulinemic conditions (Fig. 3). Adipocyte monocultures and co-cultures exhibited increased proliferation compared to day 0 during culture ($^{*}p < 0.05$). There were no significant differences between insulin conditions, and endothelial monocultures showed a decrease in DNA content over time, with no significant differences between insulin levels.

At day 9, hyperinsulinemic cultures were switched to normal insulin levels, as marked by dotted line on all plots. In co-culture (Fig. 3A), DNA content decreased after change in insulin condition, whereas normal insulin cultures continued to increase. In adipocyte monocultures (Fig. 3B), DNA content was unaffected by the change in insulin conditions after 3 days. Finally, endothelial monocultures (Fig. 3C) did not exhibit significant change after change in insulin concentration.

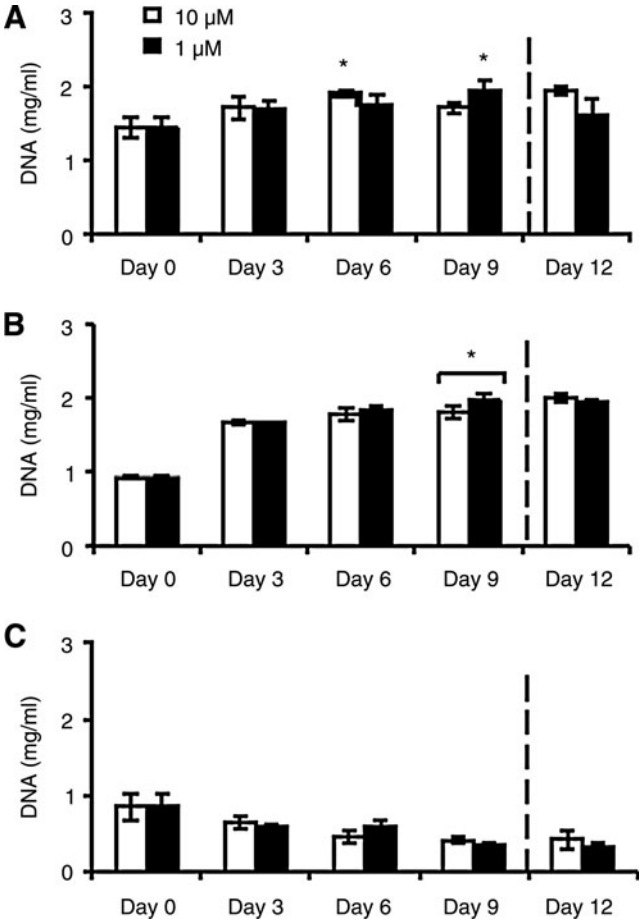

FIG. 3. DNA content of 3D constructs in the medium containing 10 or 1 μM insulin. (**A**) Adipocyte/endothelial co-cultures, (**B**) adipocyte monocultures, and (**C**) endothelial monocultures were evaluated ($n = 3$). Significant differences from day 0 levels are labeled as $^{*}p < 0.05$.

TG accumulation

In 3D adipocyte mono and co-cultures, intracellular TG levels peaked under hyperinsulinemic conditions at days 3 and 6, respectively (Fig. 4A, B). Specifically, in co-cultures (Fig. 4A), hyperinsulinemic cultures exhibited a decrease in TG content from day 0 to 3, but peaked at day 6, and then declined again at day 9. Co-cultures in normal insulin conditions, however, showed a progressive decline in TG to day 9 ($^{*}p < 0.05$). In adipocyte monocultures (Fig. 4B), both normal and hyperinsulinemic cultures followed similar trends; however, a statistical increase in TG accumulation from day 0 to 3, followed by a decline in TG by day 9 in hyperinsulinemic cultures, was observed ($^{*}p < 0.05$). Finally, endothelial monocultures cultured in both normal and hyperinsulinemic conditions were evaluated for TG content (Fig. 4C). TG was detected at basal levels, and was similar between the two insulin conditions.

Upon switching hyperinsulinemic cultures to normal insulin conditions at day 9, adipocyte co-cultures continued to decrease in TG content, whereas adipocyte monocultures exhibited an increase in TG level (Fig. 4A, B). All normal insulin cultures along with endothelial monocultures maintained TG levels at day 12. By day 12, TG levels of all constructs, those cultured in both normal and hyperinsulinemic conditions, reached similar levels.

Glycerol secretion

Secreted glycerol was measured in all constructs as a measure of basal lipolysis (Fig. 4D–F). In adipocyte co-cultures (Fig. 4D), glycerol levels were lower in hyperinsulinemic cultures than normal cultures on days 0, 3, and 6. However, at day 9, hyperinsulinemic cultures increased glycerol secretion, whereas glycerol secretion in normal insulin cultures declined. In adipocyte monocultures (Fig. 4E), glycerol levels remained relatively constant during culture, and there were no significant differences between normal and hyperinsulinemic conditions. Finally, all endothelial monocultures exhibited basal glycerol levels throughout culture (Fig. 4F).

Glycerol content after change in hyperinsulinemic cultures to normal insulin conditions did not result in any significant changes in secreted glycerol after 3 days for all constructs. Normal insulin constructs, however, exhibited increased glycerol secretion at day 12 compared to that of day 9. Endothelial monocultures exhibited basal levels throughout culture.

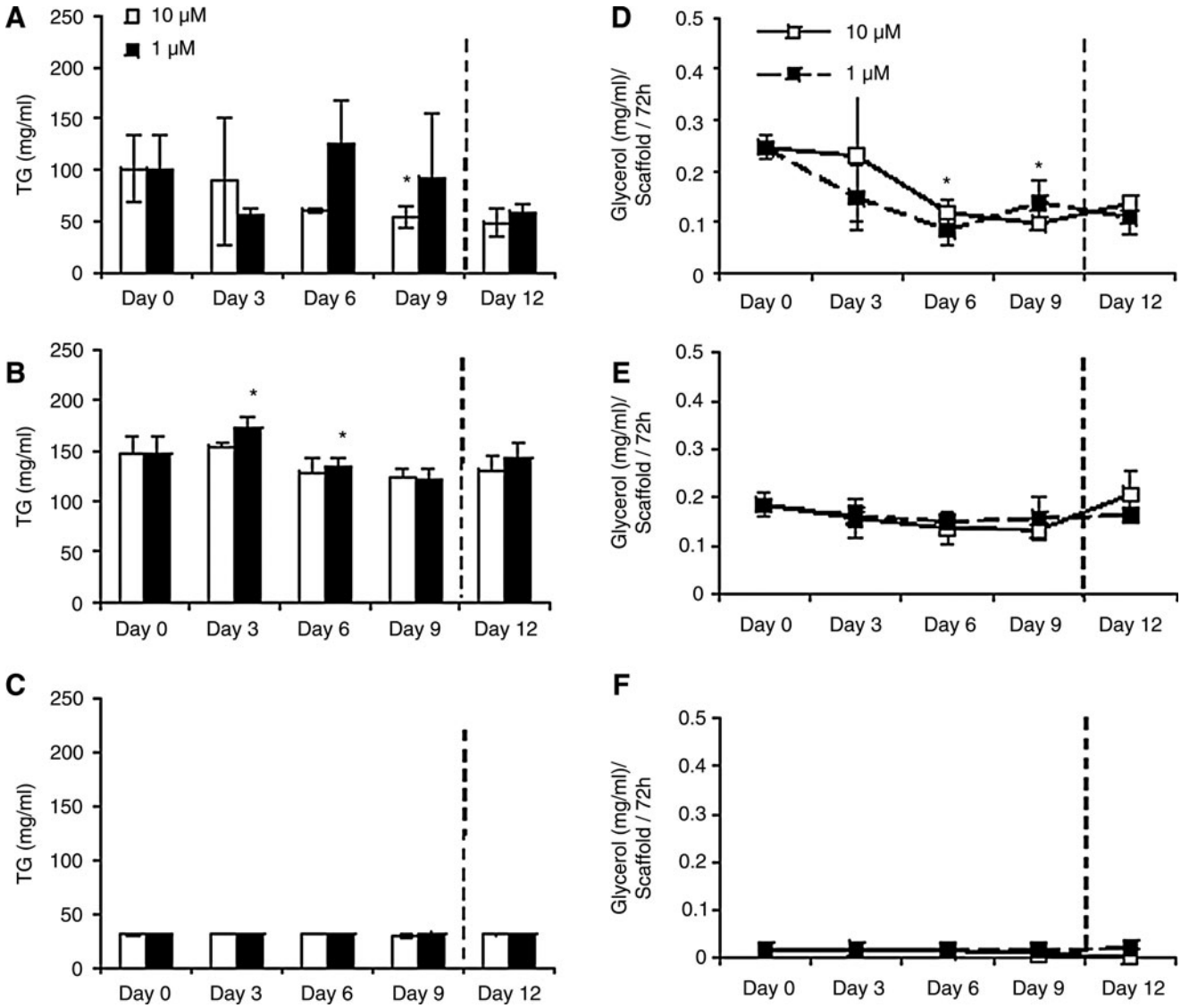

FIG. 4. Triglyceride accumulation and secreted glycerol measurements of 3D constructs cultured in medium containing 10 μM or 1 μM insulin. (**A, D**) adipocyte/endothelial co-cultures, (**B, E**) adipocyte monocultures, and (**C, F**) endothelial monocultures were evaluated ($n = 3$). Significant differences from day 0 levels labeled as $^*p < 0.05$.

Transcript expression

Glut4 transcript expression was evaluated for all constructs (Fig. 5). The hASC/HUVEC co-cultures exhibited different *Glut4* trends than monocultures (Fig. 5A). In co-culture, constructs cultured in either normal or hyperinsulinemic conditions increased *Glut4* expression with time. By day 9, both normal and hyperinsulinemic cultures significantly increased *Glut4* expression compared to day 0 levels ($^*p < 0.05$). The ASC monocultures (Fig. 5B) maintained under normal insulin conditions exhibited a gradual decline in *Glut4* expression from day 0 to 6 ($^*p < 0.05$); however, by day 9, *Glut4* increased, reaching a peak in expression. Hyperinsulinemic conditions followed a similar trend as normal insulin cultures, in which by day 6, glycerol secretion had significantly declined from day 0 levels ($^*p < 0.05$). Endothelial monocultures consisted of lower *Glut4* expression than adipocyte mono and co-cultures, and remained at a relatively consistent level throughout culture (Fig. 5C).

Upon switching hyperinsulinemic cultures to normal insulin media, ASC/HUVEC co-cultures exhibited an increase in expression by day 12 and monocultures resulted in undetectable *Glut4* expression after 3 days. Endothelial monocultures retained basal levels after change in insulin concentration.

The endothelial marker, *CD31*, was also measured as an indicator of endothelial cells in co-culture. As expected, *CD31* expression was undetectable in adipocyte monocultures, and was at peak levels in endothelial monocultures (Fig. 5D–F). Adipocyte co-cultures (Fig. 5D) expressed *CD31* throughout the culture period; however, levels were greatest at day 0. *CD31* expression then continued to decrease by day 9 ($^*p < 0.05$). In both endothelial monocultures and hASC/HUVEC co-cultures, *CD31* expression was similar in normal insulin exposure to that of hyperinsulinemic conditions. *CD31*

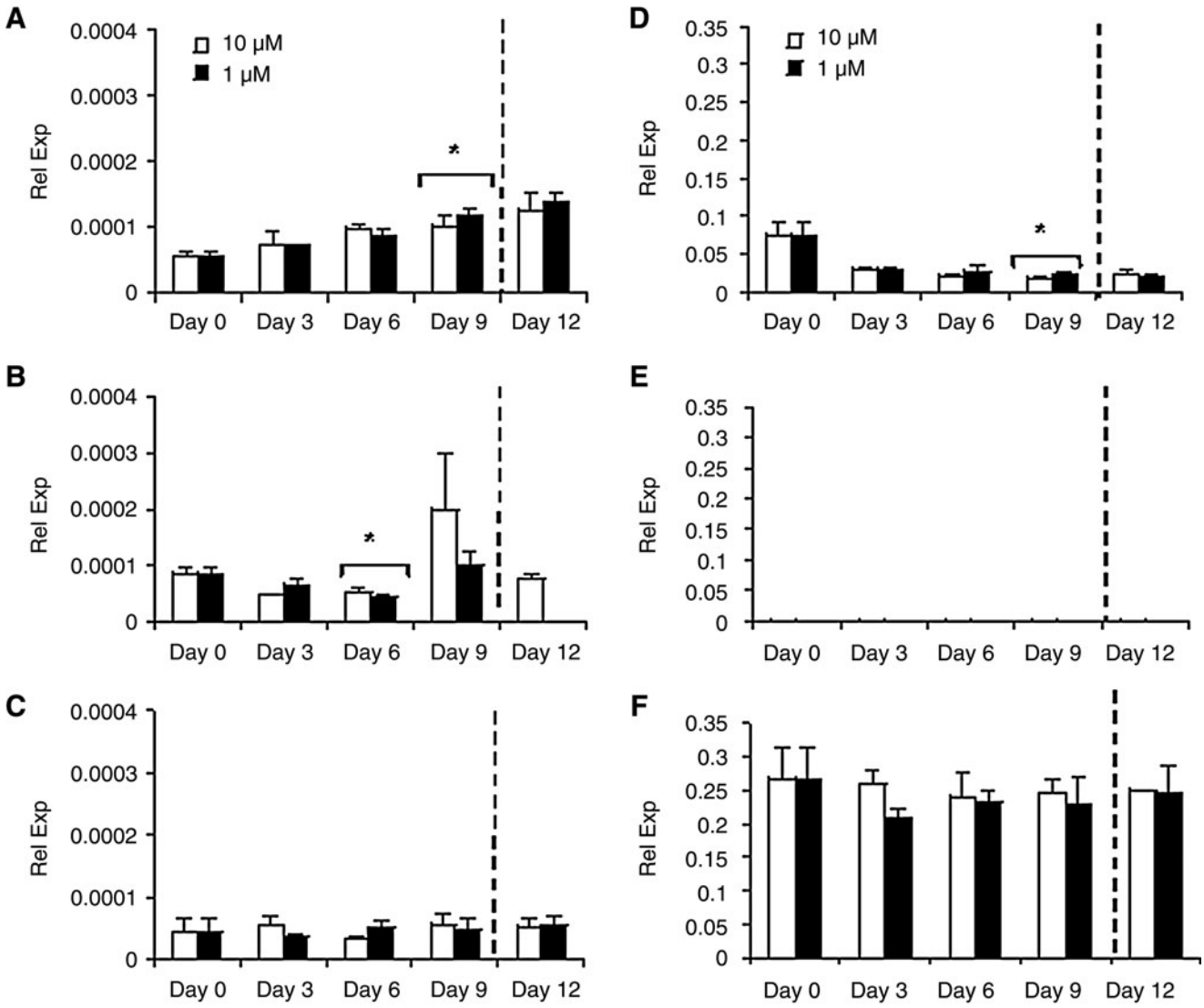

FIG. 5. Real time reverse transcription (RT)-PCR measurements for glut4 and CD31 transcript expression of 3D constructs cultured in medium containing 10 μM or 1 μM insulin. (**A, D**) adipocyte/endothelial co-cultures, (**B, E**) adipocyte monocultures, and (**C, F**) endothelial monocultures were evaluated ($n = 3$). Significant differences from day 0 levels are labeled as $^*p < 0.05$.

transcript expression after change in hyperinsulinemic cultures to normal insulin conditions did not result in any significant changes after 3 days for all constructs.

Discussion

In this study, 3D hASC/HUVEC co-cultures exhibited a differential response to hyperinsulinemic as compared to normal insulin levels, which was absent in 3D hASC monocultures. Greater TG accumulation and inhibited basal lipolysis levels were evident in co-cultures, whereas monocultures did not exhibit these physiological trends. This implies that 3D co-cultures provide a more robust *ex vivo* model for human adipose tissue biology compared to 3D adipocyte monocultures.

Understanding hyperinsulinemia is of great importance both biologically and clinically. The majority of *in vitro* studies of hyperinsulinemia and its role in insulin resistance have been conducted using 2D cell culture studies and as clinical studies.[12,14,15] We propose here an approach to study hyperinsulinemia under biologically relevant yet controllable conditions, by co-culture of adipose and vascular cells in a 3D setting. This is, to the best of our knowledge, the first report demonstrating the physiological effects of hyperinsulinemia in 3D tissue-engineered adipose constructs.

The use of 3D systems provides significant advantage over traditional 2D cultures as they provide a microenvironment for cells to adhere to, proliferate, and mature,[16] which is more representative of the native cell microenvironment. Silk fibroin scaffolds in particular have been previously shown to support adipose tissue formation.[20] Thus, investigating physiological responses to hyperinsulinemia in 3D studies may provide significant insight into mechanisms observed *in vivo* that may not have been evident in 2D models, as well as serve as a potential tissue model in which adipose-related therapies can be developed and tested.

In the current study, we have exposed 3D tissue-engineered adipose constructs to both normal insulin culture conditions (1 μM) and hyperinsulinemic conditions (10 μM). We specifically looked at hASC monocultures and hASC/HUVEC co-cultures on 3D silk fibroin scaffolds, as recently reported.[17] We evaluated the effects that insulin has on various aspects of lipogenesis and lipolysis. There are very limited reports of adipocyte/endothelial co-cultures[17,21]; however, the addition of endothelial cells into our culture system serves an important role. Endothelial co-culture strengthens our system not only in a physiological manner, as endothelial cells make up the vast capillary network of native adipose tissue,[22] but also in a biochemical manner, as endothelial cells are also affected in T2DM and obesity.[23] Specifically, endothelial dysfunction, primarily due to an altered balance in vasodilator and vasoconstrictor factor secretion by endothelial cells, has often preceded T2DM.[23,24] Endothelial dysfunction, characterized by a reduction in nitric oxide bioactivity, observed in the insulin-resistant state has been shown to be closely related to adipose tissue secretion of proinflammatory cytokines and increased free fatty acid levels.[24–26]

We initially conducted baseline studies in 2D hASC monocultures. We were interested in establishing an experimental design such that hyperinsulinemic effects that have been previously reported in 2D could be exhibited in our hASC culture system. Insulin is known to both stimulate recruitment of glucose transporters[27] and have an antilipolytic effect in adipocytes.[11] Therefore, in our studies, we cultured differentiated adipocytes for 12 days, and investigated lipid accumulation and glycerol secretion in normal (1 μM) and high (10 μM) insulin levels (Fig. 2). These levels were chosen, as 1 μM is the concentration typically found in adipocyte induction media for hASCs, and *in vivo* hyperinsulinemia levels typically range from 5 to 10 times that of normal levels[9]; thus, we chose 10 μM as the high insulin condition in our cultures. We found that adipocytes in both insulin conditions accumulated lipid to a similar degree through day 9 culture (Fig. 2). However, we notice a significant decrease in lipid content by day 12 in 10 μM cultures (Fig. 2D) compared to 1 μM (Fig. 2H). To further explain the observations, we measured glycerol secretion by adipocytes over the culture period (Fig. 2I). We saw a physiological effect, in that hyperinsulinemic cultures resulted in less glycerol secretion compared to normal insulin cultures. This remained consistent throughout the 12 days of culture, with day 6 having the greatest difference in glycerol levels. We speculate that adipocytes cultured in hyperinsulinemic conditions were beginning to gain insensitivity toward insulin, thereby increasing glycerol secretion, as lipolysis is less inhibited in the insulin resistant state.[12] Therefore, as a result, we see glycerol levels increasing with time, and lipid content decreased at day 12 possibly due to a deficiency in insulin-mediated *Glut4* membrane recruitment.[28]

Once establishing that in 2D, hASC-differentiated adipocytes responded in a physiological manner to both insulin levels, we proceeded to our 3D adipose tissue system. We investigated effects that insulin levels may have on proliferation (Fig. 3). In co-cultures, we observed that hyperinsulinemic conditions may have caused a slight lag in proliferation compared to 1 μM insulin, as hyperinsulinemic adipocytes proliferated to a significant extent by day 9, and 1 μM adipocytes reached their peak earlier, at day 6 (Fig. 3A). Adipocyte monocultures, however, exhibited similar trends in both insulin levels (Fig. 3B), and endothelial monocultures showed a decrease in DNA content over time, with no differences between insulin conditions (Fig. 3C). The presence of endothelial cells in co-culture constructs therefore may suggest that endothelial cells contribute to the hyperinsulinemic effect we see *in vivo*.

Interestingly, as with proliferation, we observed differences in TG accumulation and glycerol secretion in co-cultures, but it was not as evident in adipocyte and endothelial monocultures. Specifically, in co-culture, we observed differences in TG accumulation profiles between hyperinsulinemic and normal insulin cultures (Fig. 4A). Co-cultures in normal insulin media exhibited a gradual decline in TG content through day 9, whereas hyperinsulinemic cultures exhibited a decline at day 3, followed by an increase at day 6 and slight decline again by day 9 (Fig. 4A). Correlating this to glycerol levels (Fig. 4D), we see that in normal insulin cultures, glycerol levels continued to decline through day 9 culture, whereas hyperinsulinemic cultures declined to day 6, before increasing at day 9. In hyperinsulinemic cultures, glycerol levels reached a minimum when TG levels were at its peak. This is indicative of the dual role insulin has in adipocytes, which is to inhibit lipolysis, therefore decreasing glycerol secretion, and stimulate TG accumulation through *Glut4* membrane recruitment. *Glut4* transcript expression did not exhibit similar profiles to either TG or glycerol, but instead increased steadily over the culture period (Fig. 5A). This suggests that varying insulin levels may in fact directly impact *Glut4* at the protein level versus at the transcript level.[12]

In adipocyte monocultures, normal insulin levels did not impact TG content to a significant extent, as TG levels remained relatively constant during the culture period (Fig. 4B). Hyperinsulinemic cultures, however, exhibited a significant increase in TG at day 3, and a gradual decline for the remainder of culture. Glycerol secretion was not as distinct as it was in co-cultures, in that glycerol levels did not fluctuate significantly throughout the culture (Fig. 4E). *Glut4* transcript expression in adipocyte monocultures declined in expression at day 6 for both insulin conditions, and an increase in expression at day 9 (Fig. 5B). Further studies need to be conducted to understand the mechanisms of this response. Endothelial monocultures, as expected, consisted of a basal level of both TG and glycerol throughout culture (Fig. 4C, F). Likewise, *Glut4* transcript expression remained at low levels throughout culture (Fig. 5C). This confirmed that while endothelial cells may have played a role in hyperinsulinemic effects on adipocyte TG accumulation and glycerol secretion in co-culture, they did not themselves accumulate significant TG or secrete glycerol to a significant extent.

Finally, at day 9, we switched all hyperinsulinemic cultures to medium containing normal insulin levels (1 μM) and cultured for 3 additional days. We observed that the change in insulin concentration did not significantly affect DNA content in all three groups. While TG content remained similar in normal insulin cultures, hyperinsulinemic cultures

decreased in both TG content and glycerol release upon switching insulin levels (Fig. 4A, D). However, adipocyte monocultures exhibited an increase in TG content and glycerol secretion after the change from hyper to normal insulin levels.

In our 3D system, hyperinsulinemia (high insulin culture conditions) affected adipocyte lipogenesis and lipolysis in co-culture with endothelial cells to a greater extent than in monoculture. We demonstrated that the co-culture of adipocytes with endothelial cells was necessary for observing a physiological response to hyperinsulinemia with respect to both TG accumulation and basal glycerol secretion. The 3D adipocyte monocultures, however, did not exhibit significant differential effects in response to normal or high insulin levels, suggesting that endothelial cells play a vital role in establishing physiologically relevant responses in this 3D adipose tissue system. Future studies would involve investigating long-term effects of high insulin levels on adipocyte function, as well as studies to further elucidate endothelial contributions and more specifically that of endothelial dysfunction in the hyperinsulinemic state. The work presented here brings us a significant step forward in the development of a 3D *in vitro* adipose tissue system for detailed studies of disease and therapeutic options.

Acknowledgments

We thank the NIH P41 Tissue Engineering Resource Center (P41 EB002520) and AFIRM for support of aspects of research on soft tissue engineering.

Disclosure Statement

No competing financial interests exist.

References

1. Guilherme, A., Virbasius, J.V., Puri, V., and Czech, M.P. Adipocyte dysfunctions linking obesity to insulin resistance and type 2 diabetes. Nat Rev Mol Cell Biol **9,** 367, 2008.
2. Kahn, S.E., Hull, R.L., and Utzschneider, K.M. Mechanisms linking obesity to insulin resistance and type 2 diabetes. Nature **444,** 840, 2006.
3. Foster-Schubert, K.E., and Cummings, D.E. Emerging therapeutic strategies for obesity. Endocr Rev **27,** 779, 2006.
4. Cohen, A., and Horton, E.S. Progress in the treatment of type 2 diabetes: new pharmacologic approaches to improve glycemic control. Curr Med Res Opin **23,** 905, 2007.
5. Levetan, C. Oral antidiabetic agents in type 2 diabetes. Curr Med Res Opin **23,** 945, 2007.
6. Arner, P. The adipocyte in insulin resistance: key molecules and the impact of the thiazolidinediones. Trends Endocrinol Metab **14,** 137, 2003.
7. Iozzo, P., Pratipanawatr, T., Pijl, H., Vogt, C., Kumar, V., Pipek, R., Matsuda, M., Mandarino, L.J., Cusi, K.J., and DeFronzo, R.A. Physiological hyperinsulinemia impairs insulin-stimulated glycogen synthase activity and glycogen synthesis. Am J Physiol Endocrinol Metab **280,** E712, 2001.
8. Weyer, C., Hanson, R.L., Tataranni, P.A., Bogardus, C., and Pratley, R.E. A high fasting plasma insulin concentration predicts type 2 diabetes independent of insulin resistance: evidence for a pathogenic role of relative hyperinsulinemia. Diabetes **49,** 2094, 2000.
9. Polonsky, K.S., Given, B.D., and Van Cauter, E. Twenty-four-hour profiles and pulsatile patterns of insulin secretion in normal and obese subjects. J Clin Invest **81,** 442, 1988.
10. Weiss, P.A., Haeusler, M., Tamussino, K., and Haas, J. Can glucose tolerance test predict fetal hyperinsulinism? BJOG **107,** 1480, 2000.
11. Cimmino, M., Agosto, A., Minaire, Y., and Geloen, A. *In situ* regulation of lipolysis by insulin and norepinephrine: a microdialysis study during euglycemic-hyperinsulinemic clamp. Metabolism **44,** 1513, 1995.
12. Fernandez-Veledo, S., Nieto-Vazquez, I., de Castro, J., Ramos, M.P., Bruderlein, S., Moller, P., and Lorenzo, M. Hyperinsulinemia induces insulin resistance on glucose and lipid metabolism in a human adipocytic cell line: paracrine interaction with myocytes. J Clin Endocrinol Metab **93,** 2866, 2008.
13. Renstrom, F., Buren, J., Svensson, M., and Eriksson, J.W. Insulin resistance induced by high glucose and high insulin precedes insulin receptor substrate 1 protein depletion in human adipocytes. Metabolism **56,** 190, 2007.
14. Qi, L., Saberi, M., Zmuda, E., Wang, Y., Altarejos, J., Zhang, X., Dentin, R., Hedrick, S., Bandyopadhyay, G., Hai, T., Olefsky, J., and Montminy, M. Adipocyte CREB promotes insulin resistance in obesity. Cell Metab **9,** 277, 2009.
15. Ruge, T., Lockton, J.A., Renstrom, F., Lystig, T., Sukonina, V., Svensson, M.K., and Eriksson, J.W. Acute hyperinsulinemia raises plasma interleukin-6 in both nondiabetic and type 2 diabetes mellitus subjects, and this effect is inversely associated with body mass index. Metabolism **58,** 860, 2009.
16. Gomillion, C.T., and Burg, K.J. Stem cells and adipose tissue engineering. Biomaterials **27,** 6052, 2006.
17. Kang, J.H., Gimble, J.M., and Kaplan, D.L. *In vitro* 3D model for human vascularized adipose tissue. Tissue Eng Part A **15,** 2227, 2009.
18. Dubois, S.G., Floyd, E.Z., Zvonic, S., Kilroy, G., Wu, X., Carling, S., Halvorsen, Y.D., Ravussin, E., and Gimble, J.M. Isolation of human adipose-derived stem cells from biopsies and liposuction specimens. Methods Mol Biol **449,** 69, 2008.
19. Kim, U.-J., Park, J., Kim, H.J., Wada, M., and Kaplan, D.L. Three-dimensional aqueous derived biomaterial scaffolds from silk fibroin. Biomaterials **26,** 2775, 2005.
20. Mauney, J.R., Nguyen, T., Gillen, K., Kirker-Head, C., Gimble, J.M., and Kaplan, D.L. Engineering adipose-like tissue *in vitro* and *in vivo* utilizing human bone marrow and adipose-derived mesenchymal stem cells with silk fibroin 3D scaffolds. Biomaterials **28,** 5280, 2007.
21. Lai, N., Jayaraman, A., and Lee, K. Enhanced proliferation of human umbilical vein endothelial cells and differentiation of 3T3-L1 adipocytes in coculture. Tissue Eng Part A **15,** 1053, 2008.
22. Hausman, D.B., DiGirolamo, M., Bartness, T.J., Hausman, G.J., and Martin, R.J. The biology of white adipocyte proliferation. Obes Rev **2,** 239, 2001.
23. Jansson, P.A. Endothelial dysfunction in insulin resistance and type 2 diabetes. J Intern Med **262,** 173, 2007.
24. Rask-Madsen, C., and King, G.L. Mechanisms of disease: endothelial dysfunction in insulin resistance and diabetes. Nat Clin Pract Endocrinol Metab **3,** 46, 2007.
25. Bakker, W., Eringa, E.C., Sipkema, P., and van Hinsbergh, V.W. Endothelial dysfunction and diabetes: roles of hyperglycemia, impaired insulin signaling and obesity. Cell Tissue Res **335,** 165, 2009.

26. Kearney, M.T., Duncan, E.R., Kahn, M., and Wheatcroft, S.B. Insulin resistance and endothelial cell dysfunction: studies in mammalian models. Exp Physiol **93,** 158, 2008.
27. Hauner, H., Rohrig, K., Spelleken, M., Liu, L.S., and Eckel, J. Development of insulin-responsive glucose uptake and GLUT4 expression in differentiating human adipocyte precursor cells. Int J Obes Relat Metab Disord **22,** 448, 1998.
28. Rubin, B.R., and Bogan, J.S. Intracellular retention and insulin-stimulated mobilization of GLUT4 glucose transporters. Vitam Horm **80,** 155, 2009.

Address correspondence to:
David L. Kaplan, Ph.D.
Department of Biomedical Engineering
Tufts University
Colby St.
Medford, MA 02155

E-mail: david.kaplan@tufts.edu

Received: November 25, 2009
Accepted: February 9, 2010
Online Publication Date: March 10, 2010